

LDA Measurements in the Unsteady Wake of a Multiple Fins Oscillator

A Leder, A Jianu

This paper presents experimental results from a multiple fins oscillator, which has been employed to vertically oscillate the fluid in a rectangular tank filled with water. The fins perform a combined heaving and pitching oscillation while the whole oscillating machine is stationary. The distance between two adjacent fins is regarded as the oscillator characteristic length D with $D = 0,05$ m. While applying a time-periodic forcing, flow field measurements were carried out using a two-component laser-Doppler anemometer. The measured velocity data have been phase-synchronised with the periodic excitation by sensing the position of the oscillating fins with a Hall-probe. The wakes behind the oscillating fins show time averaged velocity profiles in the form of jets. The flow pattern comprises back-flow areas in-between the fins. Concentrated vorticity regions originating from the fins extend up to a streamwise distance of approx. $0.5D$. For larger distances from the fins, the vortices become unstable and they decay into small scale vortices. At $x = 2.5D$ the turbulent fluid motions are nearly homogeneous with a turbulence intensity of $Tu \cong 25\%$.

Introduction

Stirred tanks are encountered in a variety of industrial applications (blending, dispersing liquids, chemical reactors, pre-treatment stages of metal molded article coating, etc). Flow control in tanks is currently attracting increased attention: flow destabilization (eg, for better mixing) or flow stabilisation (eg, for eliminating unsteady loads) may be desired. The techniques may be classified into two categories: passive control (by altering the flow geometry) and active control (by applying a time-dependent forcing to the flow). Active control may be divided into open-loop (forcing is a prescribed function of time) and closed-loop schemes (forcing is a function of real-time flow response measurement)¹.

Nomenclature

D	distance between two fins (length scale)
f	frequency
H	height of tank
L	length of tank
T	period of time
Tu	turbulence intensity
u^*	reference value for velocity
u	velocity-component in x-direction
w	velocity-component in z-direction

Institute of Fluidmechanics, University Rostock,
Albert-Einstein-Str. 2, D-18051 Rostock, Germany,
E-mail: alfred.leder@mbst.uni-rostock.de

W	width of tank
x,y,z	co-ordinates
ω	rotation of the flow

Subscripts

o	averaged value at $x/D = 2.5$
y	in y-direction
g	total value

Mathematical symbols

\bar{a}	time averaged value of "a"
$\langle a \rangle$	mean value of "a" at constant phase

In this paper, we report on two-dimensional LDA experiments in the outflow region of a multiple fins oscillator placed in a water tank. An active flow control in an open-loop scheme is investigated, which relies on directly generating instabilities by applying a harmonic forcing to the flow. The purpose of this study is to get an accurate knowledge of the basic fluid mechanics induced by a multiple fins oscillator.

Previously, thrust-producing harmonically flapping foils have been studied mainly to derive efficient propulsion-techniques. A moving flapping foil produces thrust through the flow formation downstream from the trailing edge, which, when averaged over the period of oscillation, has the form of a jet. This jet flow is unstable, acting as a narrow-band amplifier of perturbations. The harmonic motion of the foil causes unsteady shedding of vorticity from the trailing edge²⁻⁴. Stationary foils have also been studied as vortex splitting devices in boundary-layer control experiments⁵⁻⁷. The linear and nonlinear inviscid theories of unsteady foil flow and thrust production have been studied^{8, 9}.

The objective of the present study is to describe the time-averaged and unsteady structure of the flow field in the close vicinity of the oscillator fins for different driving frequencies. The emphasis is on the characterization of the developing flow structure and turbulence intensity¹⁰.

Fig. 1 illustrates the oscillating movement of a single fin, induced by a heaving motion of the oscillator-frame. The fin oscillates in a combined translational and rotational motion which is due to its own elasticity.

Experimental Setup

Flow facility

The flow facility is shown in Fig. 2. The rectangular tank is 240

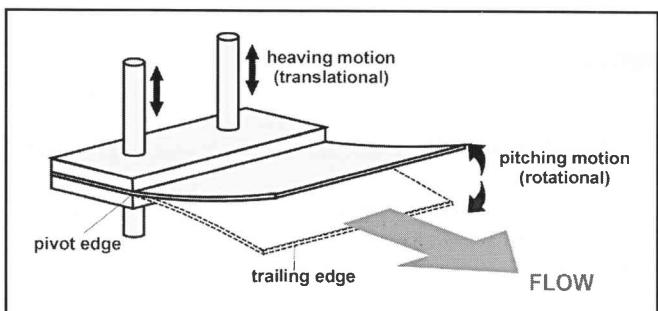


Fig 1: Oscillating motion of a single fin

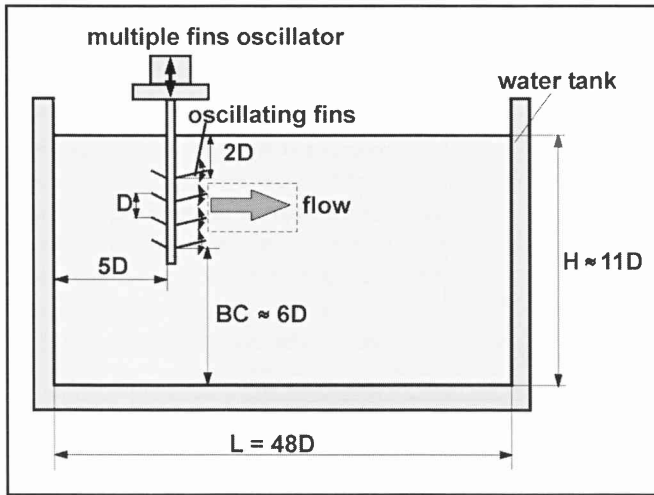


Fig 2: Sideview of rectangular water tank, ($D = 0,05$)

cm long (L) and 60 cm wide (W) and is filled with quiescent water up to a level (H) of 53 cm. At the top level there is a free surface. One of the long walls of the tank is equipped with a glass window.

A four-fins oscillator was mounted in the vicinity of one of the short walls of the tank, with a bottom clearance BC (distance from the lowest fin to the tank bottom) equal to 28 cm and a top clearance TC (distance from the top fin to the free water surface) equal to 10 cm. The fins are 25 cm long, 5.5 cm wide and 0.08 cm thick. The distance between two adjacent fins is regarded as the oscillator characteristic length, $D = 5$ cm. The fins oscillate in a combined translational (heave) motion (forced by the vibrating motor) and rotational (pitch) motion due to their own elasticity. Fig 3 illustrates the multiple fins oscillator used for these experiments.

LDA set-up

The optics of the 2D LDA set-up consists of a 500 mW Ar-ion laser, a transmitter box, a 2D probe based on the colour separation method and two photo-multipliers. The 2D probe and the transmitter box are linked by glass fibers. The transmitter contains a colour separator and a frequency shifting Bragg cell. Its primary function is to extract two mono-frequency colors



Fig.4: Sideview of the oscillator and look at the four laser beams of the 2D LDA-optics

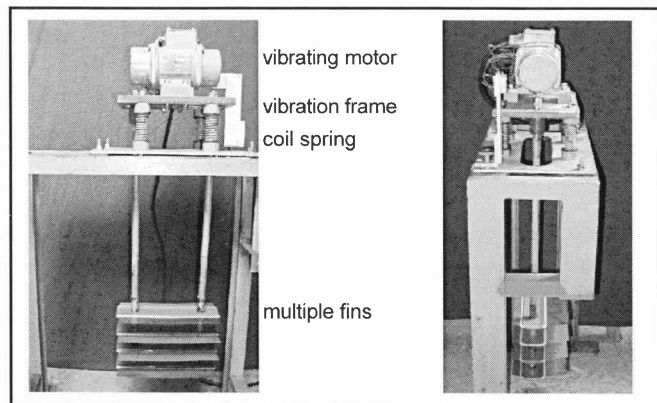


Fig.3: Front and sideview of a four step fins oscillator

from the laser beam and to split each color into two beams with a 40 MHz frequency difference. Here the 514.5 nm and 488 nm color lines have been used. Two Burst Spectrum Analyzers (BSA) process the signals from the photo-multipliers. The BSA's are interfaced to a microcomputer by GPIB interface and BSA Flow software. The measured LDA data have been phase-synchronized with the periodic actuator movement by sensing the position of the fins with a Hall-probe mounted on the frame of the oscillator. The beginning of every cycle, as detected by the Hall-probe, was time-stamped by a TTL impulse and inserted into the series of arrival time records of the validated LDA data¹⁰.

Data acquisition

A measurement grid (Fig. 5) was defined in the vertical plane (perpendicular to the fins) horizontally placed on the center line of the set-up. A Cartesian co-ordinate system is used with the origin (O) at the midpoint between the two lower fins. The (x, z)

axes are directed streamwise (horizontal and vertical, respectively). The component of the velocity vector in x -direction is defined as u , in z -direction as w -component.

The probe was mounted on a 2D traverse system for accurate positioning of the measuring volume on the measurement grid. The traversing system was computer-controlled by a microcomputer linked with the BSA computer through a serial interface. BSA Flow software communicated with the traverse system through a custom-made interface software.

The grid spacing in both directions is $\Delta x = \Delta z = 0.1D$ (546 measurement points).

Geometrical variables are normalized with the oscillator characteristic length D , velocity-values with the mean streamwise velocity u_{O}^* , calculated by an integration of the u -component over the z -co-ordinate at $x/D = 2.5$. Samples $1500 \div 8000$ have been acquired per measurement position, depending on the location of the measuring volume on the grid.

Results and Discussion

As the flow pattern in the tank depends closely on the type of stirrer, detailed knowledge of the hydrodynamics close to the oscillator is important. The flow field has been measured at 37 Hz, 40 Hz and 43 Hz motor driving frequencies. The next chapter summarizes characteristic results at a forcing frequency of 40 Hz.

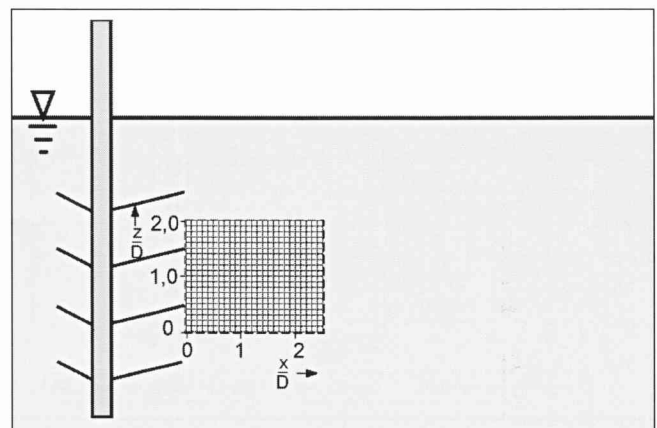


Fig.5: Measuring grid within the stirred tank

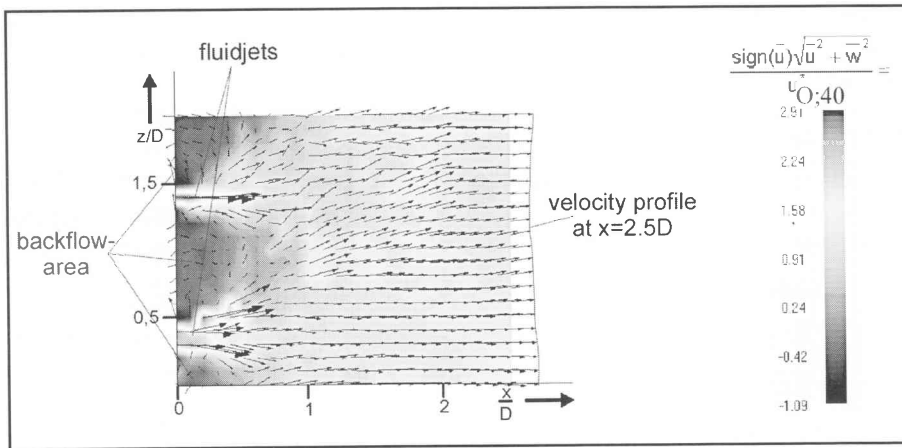


Fig. 6: Time averaged flow velocity, induced by the multiple fins oscillator $u_{O;40}^* = 0,55 \text{ m/s}$

Flow field at 40 Hz motor driving frequency

The structure of the mean flow is shown in Fig. 6. In this Fig the u -signed absolute mean velocity

$(\text{sign}(u) \cdot [\sqrt{u^2 + w^2}] / u_O^*)$ and uw -velocity vectors are plotted.

The flow pattern comprises three back-flow regions (above the upper fin, below the lower fin and inbetween the fins), extending in x direction up to a distance of approx. $0.5 D$. Further downstream there exists no back-flow. The main flow is directed horizontally. At $x/D = 2.5$ the velocity profile shows nearly no velocity gradient in z -direction.

As already reported in literature², the wake behind an oscillating foil has an average velocity profile with the form of a jet. Two jets generated by the two fins can be noticed in Fig. 6 and Fig. 7. Consequently, the mean velocity profiles in Fig. 7 for $x < 1 D$ are characterised by two positive peaks. There exists an offset between peak positions (positions of the jet origin) and the position of the trailing edges of the fins while the vibrating machine is off. Under operation, the vibration shafts are slightly pushed backward (their working position is slightly deviated from the vertical one) also causing a change in the fins position. With increasing x , the peaks decrease in amplitude and are getting broader. For $x > 1.5 D$ the profiles approach a constant value which slightly decreases with increasing x .

The fins oscillations induce an unsteady flow. The harmonic motions of the trailing edges produce periodical velocity variations within the fluid, which are resolvable with the phase locked LDA technique¹⁰. To discuss the flow dynamics one

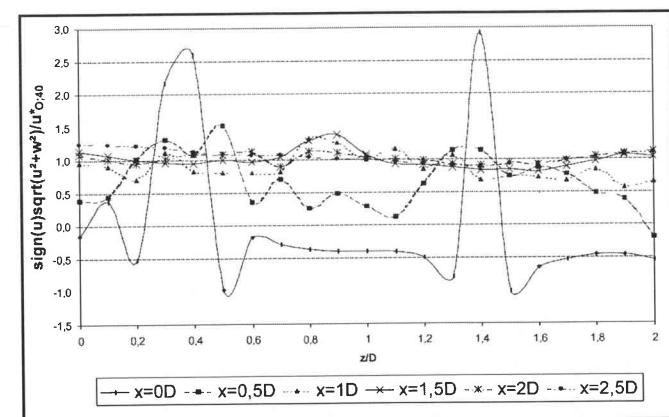


Fig. 7: Development of velocity profiles; $u_{O;40}^* = 0,55 \text{ m/s}$

period of the fins oscillations have been resolved into 10 time steps. The periodically repeated process with a duration of $T = 0.025$ seconds is thus represented by a frame sequence in which neighboring frames represent mean values of the represented flow quantity at constant phase with a temporal shift of $\Delta t = 2.5 \text{ ms}$. Fig 8 represents the fluid vorticity ω_y around the y -axis of the co-ordinate system. The brackets symbolise mean values at constant phase:

$$\langle \omega_y \rangle = \frac{\partial \langle u \rangle}{\partial z} - \frac{\partial \langle w \rangle}{\partial x}$$

Fig 8 clarifies that the fins oscillations induce within one period or 0.025 seconds one clockwise (grey, ω positive) and one counter clockwise (black, ω negative) rotating vortex structure. The vortex structures are shifted approx. $0.5 D$ downstream in x -direction which corresponds with a mean transport velocity of 1.0 m/s . Interactions between the counter rotating regions induce instabilities resulting into decomposition processes of the large scale vortices. Downstream of $x = 1 D$ small scale vortices with a diameter of approx. $0.2 D$ could be identified. With increasing x -co-ordinate $|\omega_y|$ decreases.

Fig 9 displays the arithmetic mean of both measured turbulent velocity components u' and w' , normalised with the reference velocity $u_{O;40}^*$. Tu_y represents the along the z -co-ordinate averaged turbulence intensity. Obviously Tu_y reaches a maximum value of 80% at $x = 0.5 D$. At this position the decay processes of the large scale vortices start. Between $0.5 \lesssim x/D \lesssim 1.0$ Tu_y decreases with a steep slope. In the region $x > 1.0 D$, where small scale vortices dominate the flow, the slope becomes less steep. At $x/D = 2.5$ the mean turbulence intensity is 24% .

Influence of motor driving frequency on the flow field characteristics

Measurements have been performed at two more oscillator frequencies, at $f = 37 \text{ Hz}$ and $f = 43 \text{ Hz}$. Table 1 shows the dependence of the reference velocity $u_{O;40}^*$: Increases with the increasing frequency of the multiple fins oscillator.

The developing flow features in the form of fluid jets, large scale vortices, and the decay process are very similar and show no remarkable frequency dependence. Fig 10 illustrates the time

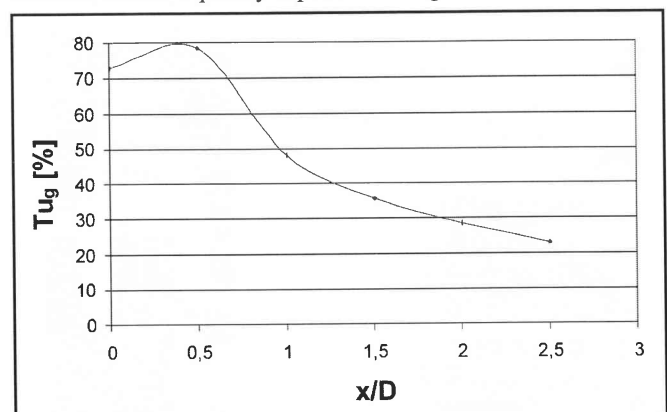


Fig. 9: Variation of the turbulence intensity Tu_y along the x co-ordinate

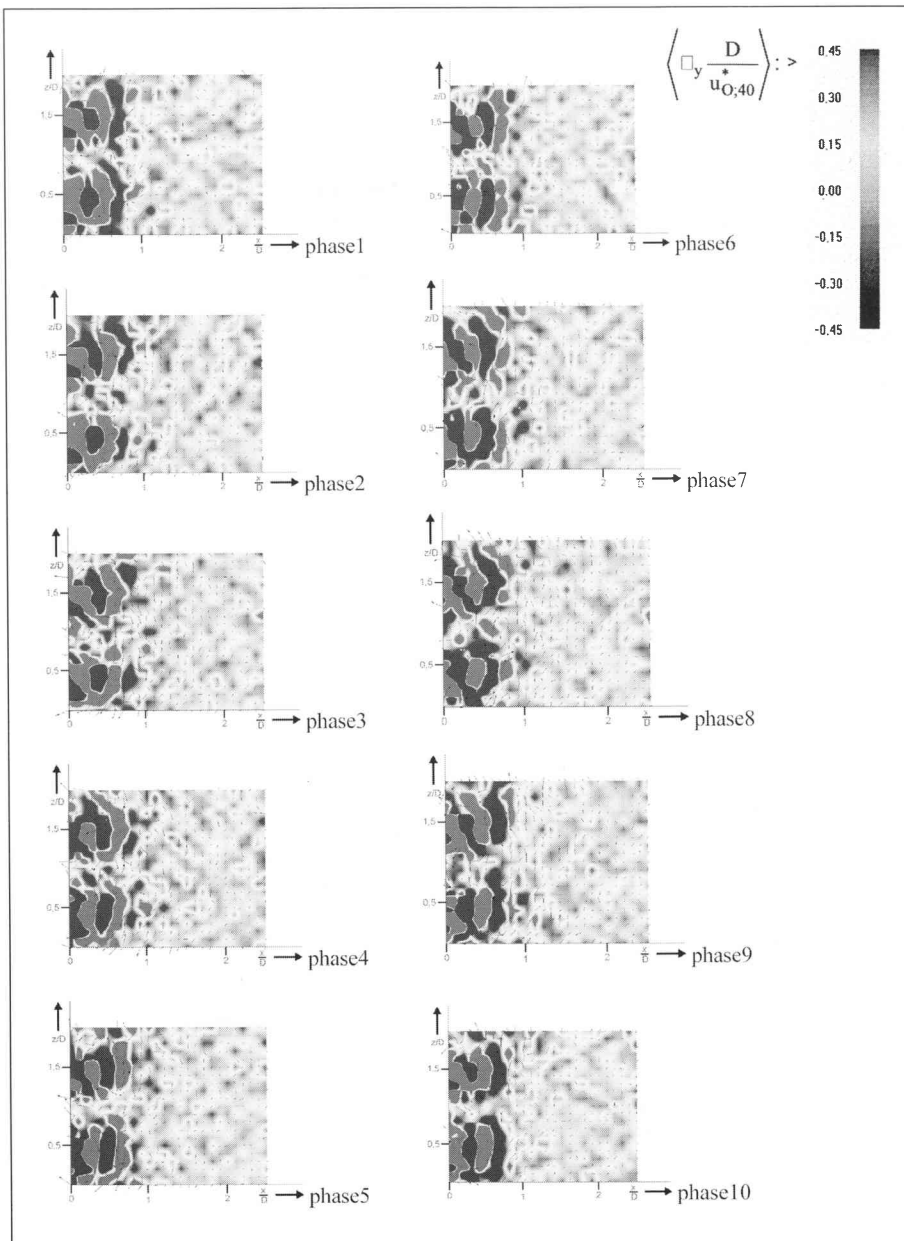


Fig. 8: Phases 1-10 of fluid rotation $\langle \omega_y \rangle$

averaged velocity profiles at two different positions ($x/D = 0.0$ and $x/D = 2.5$). Normalised with the reference velocities of Tab.1 the curves in Fig. 10 are qualitatively and quantitatively nearly identical.

Similar statements can be deduced for the behaviour of the

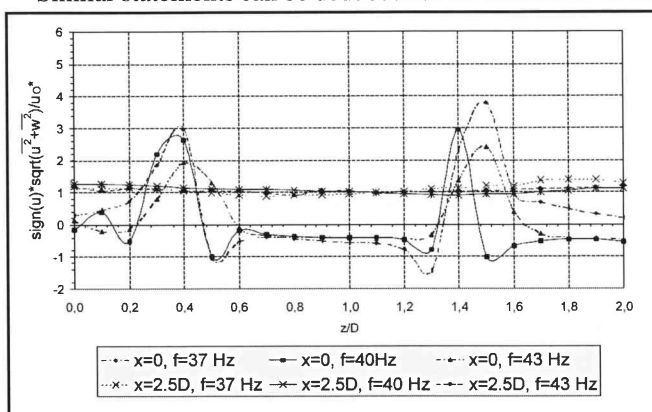


Fig. 10: Induced velocity profiles at the positions $x/D = 0.0$ and $x/D = 2.5$ at the frequencies $f = 37\text{ Hz}$, $f = 40\text{ Hz}$ and $f = 43\text{ Hz}$

turbulence characteristics: in normalising the mean of the turbulent velocity components u' and w' with the frequency dependent reference velocity, a nearly identical distribution of Tu_g results. At $x/D = 2.5$ for all three frequencies Tu_g reaches a constant value of $25\% \pm 3\%$.

Conclusions

The objective of the present report was the description of the time-averaged and unsteady flow field close to a multiple fins oscillator (up to a streamwise distance of $2.5D$) in terms of mean velocity, mean values at constant phases, and turbulence intensity. The flow pattern comprises areas of backward flow in-between the fins (extending up to a streamwise distance of $0.5D$). The main flow is horizontally directed. Turbulence intensity, and spanwise vorticity have significant values in the near vicinity of the trailing edges of the fins (up to a streamwise distance of approx. $0.5D$). Further downstream interaction processes between clockwise and counter clockwise evident rotating large scale vortices which induce instabilities leading to small scale vortices. The overall features of the flow field (flow structure, turbulence intensity, vorticity) are nearly independent from the excitation frequency by scaling with $u_O^* \cdot u_O^*$ increases with increasing driving frequency (Tab. 1).

Acknowledgement

The authors thank Japan Techno Co, Ltd, Ryushin Omasa, as well as HJ Speck (DaimlerChrysler AG) and P Claude (Chemetall) for supporting this study.

References

1. R Gopalkrishnan, MS Triantafyllou, GS Triantafyllou and DS Barrett, Active vorticity control in a shear flow using a flapping foil, *J Fluid Mech*, vol. 274, pp. 1-21, 1994.
2. MS Triantafyllou, GS Triantafyllou and R Gopalkrishnan, Wake mechanics for thrust generation in oscillating foils, *Physics of Fluids A*, vol. 3(12), pp. 2835-2837, 1991.
3. K Streitlien, GS Triantafyllou and MS Triantafyllou, Efficient foil propulsion through vortex control, *AIAA Journal*, vol. 34 (11), pp. 2315-2319, 1996.
4. JM Anderson, *Vortex Control for Efficient Propulsion*, Ph.D thesis, Mass.Inst. of Techn, Cambridge, Mass, 1996

u_O^* [m/s]	37 Hz	40 Hz	43 Hz
$u_O^* =$	0,37	0,55	0,62

Tab 1: Frequency dependence of reference velocity u_O^*

5. TC Corke, YG Guezennec and HM Nagib, *Modification in drag of turbulent boundary layers resulting from manipulation of large-scale structures*, Proc. Viscous Drag Reduction Symp. Dallas AIAA Prog. Astro. Aero. vol. 72, pp. 128-143, 1979.
6. JN Hefner, LM Weinstein and DM Bushnell, *Large-eddy break-up scheme for turbulent viscous drag reduction*, Proc. Viscous Drag Reduction Symp. Dallas AIAA Prog. Astro. Aero. vol. 72, pp. 110-127, 1979.
7. AP Dowling, *The effect of large eddy break-up devices on oncoming vorticity*, J Fluid Mech, vol. 160, pp. 447-463, 1985.
8. TY Wu, *Hydromechanics of swimming propulsion*, J Fluid Mech. vol. 46, pp. 337-335, 1971.
9. MG Copra, J Fluid Mech. vol. 74, pp. 161, 1976.
10. A Leder, *Abgelöste Strömungen – Physikalische Grundlagen*, Vieweg, 1992.